Interplay between Atomic and Mesoscopic Order on Gold Vicinal Surfaces

V. Repain, J. M. Berroir, B. Croset, and S. Rousset
Groupe de Physique des Solides, CNRS, Universités Paris 7 et Paris 6, 2 Place Jussieu, 75251 Paris Cedex 5, France

Y. Garreau
LURE, CNRS-MRES-CEA, Bâtiment 209D, Centre Universitaire, 91898 Orsay Cedex, France

V. H. Etgens
Laboratoire de Minéralogie et Cristallographie, CNRS, Universités Paris 6 et 7, 4 Place Jussieu, 75252 Paris Cedex 05, France

J. Lecoeur
Laboratoire de Physico-chimie des Surfaces, CNRS, ENSCP, 11 rue Pierre et Marie Curie, 75231 Paris Cedex, France
(Received 5 January 2000)

Self-organization on Au(1, 1, 1) vicinal surfaces provides a unique opportunity to study the interplay between atomic and mesoscopic order. First, experimental results demonstrate the different interactions between steps and surface reconstruction on Au(1, 1, 1) vicinal surfaces. Depending on the step atomic structure, lines of discommensurations are found to be either parallel or perpendicular to the step edges. This leads to a complete understanding of the mesoscopic self-organization on theses surfaces, which drastically depends on the step structure. This points out the crucial role played by the edge energy cost which can monitor the faceting periodicity in a wide range of values.

PACS numbers: 68.35.Bs, 05.65.+b, 61.10.–i, 68.35.Md

Self-organization on solid surfaces has been recognized as a promising alternative for growing uniform nanostructures with regular sizes and spacings [1]. Despite the fact that a great variety of systems and geometries are concerned [2–4], long range elastic interaction is the common physical driving force of this phenomenon [5]. In the case of the spontaneous periodic faceting of some stepped surfaces [5–7], the elastic strain field results from a discontinuity of the intrinsic surface stress tensor which appears on the facets frontier. A theoretical prediction is that, in such surfaces, the period results from a compromise between the energy gain induced by bulk elastic relaxation and the local energy cost of the facet edges [8]. However, despite a lot of work that has been concentrated on elastic relaxations, little is known about boundary energy terms.

The self-organization of Au(1, 1, 1) vicinal surfaces provides a unique opportunity to point out for the first time the crucial role of the boundary energy cost. It is well known that the mesoscopic order on these surfaces drastically depends on the step microstructure [7]. Long range order distances of about 200 nm are observed for surfaces with $\{1, 1, 1\}$ step edges, whereas for those with $\{1, 0, 0\}$ step edges, periods are about 7 nm. In this Letter, we determine the microscopic structure at a facet boundary for both kinds of surfaces and deduce the local boundary energy cost which is found to be strongly different for both types of vicinal surfaces. Finally, in the framework of Marchenko's model, it is shown that this difference in the boundary energy cost accounts for the observed mesoscopic morphologies. It is an illustration of how the step atomic structure interplays with the mesoscopic order in the self-organization phenomena.

The first stage of this work consists in the precise determination of the atomic arrangement for both kinds of vicinal surfaces. First, we present a complete structural determination of a Au(1, 1, 1) vicinal surface with $\{1, 0, 0\}$ steps, using grazing incidence x-ray diffraction (GIXD) and scanning tunneling microscopy (STM). The Au(11, 9, 9) surface is misoriented by an angle of 5.57° towards a $[2, \bar{1}, \bar{1}]$ azimuth. The sample is a disk of 10 mm in diameter and 2 mm in thickness, polished to a mirrorlike surface. The surface has been prepared *in situ* in a UHV chamber by repeated cycles of sputtering and annealing at a temperature of about 800 K [7]. This leads to a stable morphology, consisting of a periodic succession (period about 7 nm) of one large terrace (width $w_1 = 4.2$ nm) followed by one (structure 1) or two (structure 2) short terraces ($w_2 = 1.4$ nm) (cf. Fig. 1a). The proportion p of structure 2 is found to be about 70%. Previous investigations [7] have not evidenced any reconstruction on this surface. GIXD experiments were performed in a UHV diffractometer on beam line DW 12 at LURE-DCI.

Results of GIXD measurements are shown in Figs. 1b–1d. We use the hexagonal (H, K, L) coordinate system convenient for the (1, 1, 1) fcc terrace structure [9]. Performing H scans (scans perpendicular to the step edge) at different L values (L direction is perpendicular to the terraces) reveals that all diffraction rods are parallel and oriented perpendicular to the macroscopic surface (cf. Fig. 1b). The slope of the rods (5.7°) and the distance between them giving a periodicity of 6.9 nm are both consistent with the expected morphology shown in Fig. 1a. Surprisingly, experimental spectra, all obtained

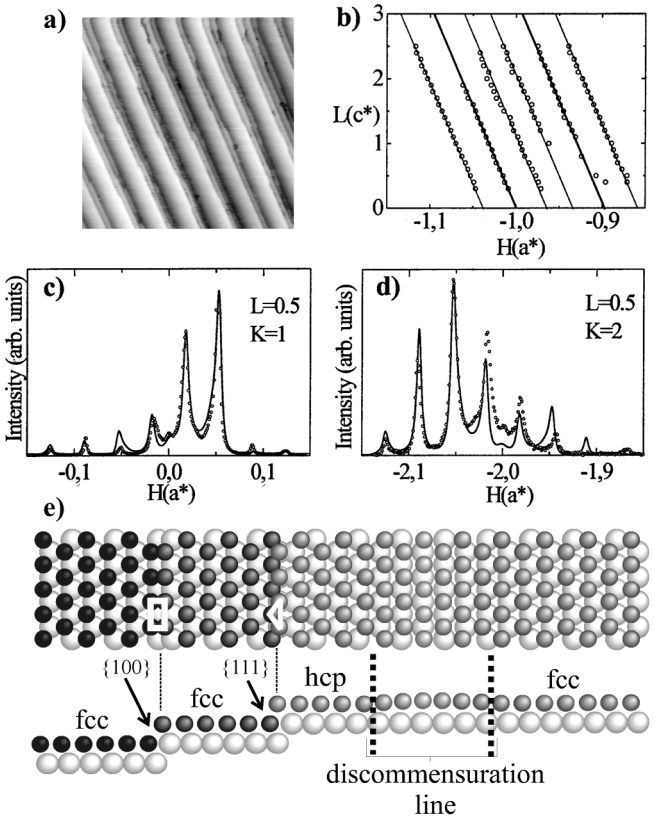

FIG. 1. Faceted Au(11, 9, 9) surface: (a) 50 nm × 50 nm STM image; all steps are of monoatomic height going downwards from bottom left to upper right; (b) H positions versus L of the main peaks observed on the H scans at $K = 2$. Straight lines are guide to the eyes; (c) and (d) the open circles display typical GIXD H-scans recorded at anti-Bragg conditions but for different values of K and L. Lines display the calculated spectra deduced from our model; (e) schematic top view (upper part) and side view (lower part) of the atomic structure showing the surface reconstruction on the large terrace. The $\{1, 0, 0\}$ step ($\{1, 1, 1\}$ step) has been highlighted by a white rectangle (triangle). The stacking sequence of topmost atoms, hcp, or fcc is indicated above each terrace.

by scanning in the anti-Bragg conditions but at different positions of the reciprocal space, drastically differ in their intensity distribution (see Figs. 1c and 1d). The origin of such a behavior has to be searched in the atomic surface structure. It is well known that on the Au(1, 1, 1) surface, topmost atoms are uniaxially compressed along one of the three equivalent close-packed directions, leading to discommensuration lines associated with the famous $22 \times \sqrt{3}$ reconstruction [10]. These lines separate regions of regular face centered cubic (fcc) stacking from regions of hexagonal close packed (hcp) faulted stacking. On the Au(11, 9, 9) surface, we did not observe any satellite peak characteristic of the usual Au(1, 1, 1)-$22 \times \sqrt{3}$ reconstruction. Following recent findings on the interaction between steps and reconstruction on a Au(1, 1, 1) surface [11], we developed an atomic model of the surface in order to reproduce the GIXD spectra. This model includes a discommensuration line parallel to the step edges on the larger terraces, which respects the surface symmetry but which is not in any usual direction known for the $22 \times \sqrt{3}$ reconstruction. In our model, atoms of the large terraces which are near the descending step are in hcp sites whereas those near the ascending step are in fcc sites (cf. Fig. 1e). The smaller terraces remain unreconstructed. Our model also includes the arrangement of structure 1 and structure 2 on the surface [12]. The terrace widths w_1 and w_2, as well as the proportion p of structure 2, have been determined by statistic over STM images. Thus, the model contains three parameters: the correlation coefficient q of the ordering between the two structures ($q = 0$ corresponds to completely segregated phases and $q = 1$ corresponds to a random mixture between the two structures), the width, and the position of the discommensuration line. As shown in Figs. 1c and 1d, the introduction of the discommensuration line accounts for the strongly different spectra obtained in the anti-Bragg condition, and the agreement between the experimental data (open circle) and the calculated spectra (full line) is excellent. Parameters deduced from the calculations are $q = 0.45$, the discommensuration line width is six atoms, the fcc (hcp) stacking domain on the large terrace contains 7 (5) atomic rows (cf. Fig. 1e).

Although this reconstruction is unusual, it is consistent with previous works on the Au(1, 1, 1) surface [11]: a discommensuration line is systematically observed parallel to the step edge at the bottom of $\{1, 0, 0\}$ steps whereas $\{1, 1, 1\}$ steps are always crossed by discommensuration lines. This was interpreted by a step energy minimization. This effect is even more important in the case of the Au(11, 9, 9) surface. Indeed, the descending step edges of the larger terraces are transformed into $\{1, 1, 1\}$ step edges (cf. Fig. 1e) which is known to be energetically favorable. The particular behavior of the reconstruction is thus strongly governed by step energetic arguments. It should also be mentioned that the existence of such stacking fault lines has been suggested on a Pt(1, 1, 1) vicinal surface with $\{1, 0, 0\}$ steps [13].

Since the period of the Au(11, 9, 9) surface is only 7 nm, it is questionable whether its morphology can be interpreted using a phase separation argument. It is necessary to conclude on this point before applying Marchenko's model to the mesoscopic order of gold vicinals, since the starting point of this model is that the surface is unstable towards faceting [8]. Since the microscopic structure of the discommensuration line (cf. Fig. 1e) found on Au(11, 9, 9) consists of a purely uniaxial compression in the direction perpendicular to the step edges, we developed a one dimensional model to demonstrate the faceting properties of this surface. Details of this calculation will be given elsewhere. The stressed terrace energy per unit area E_1 is calculated as a function of the terrace width L using a Frenkel-Kontorova (FK) model [14,15]. For simplicity, we have assumed that hcp and fcc sites are equidistant

and energetically equivalent. Furthermore, we consider the asymptotic case of infinite spring strengths, whose validity has been discussed in previous work [16]. In this case, the only boundary condition is that the first atom of the FK chain is fixed in a trough of the substrate potential (corresponding to the first atom which is not a surface atom as shown in the inset in Fig. 2). Since the fundamental FK parameter P_0 [14] which defines the misfit between the surface and the bulk atoms is not known for the Au(11, 9, 9) reconstruction, we assume that the atomic surface density should be similar to the Au(1, 1, 1) reconstructed surface and thus we take $P_0 = 22$. The graph of E_1, shown in Fig. 2, displays several minima which correspond to terrace widths locked by the reconstruction. For a vicinal surface, the surface energy per unit area also includes the step energy cost $E_2 = B/L$ and the repulsive elastic interaction energy between steps, $E_3 = C/L^3$. These contributions, where B and C have been deduced from the experimental data of Wang *et al.* [17], are also shown in Fig. 2. The curve of the total energy per unit area E clearly displays an additional minimum associated with unreconstructed terraces, 1.4 nm wide. Finally, the total energy curve is nonconvex and the tie bar construction applied to a Au(11, 9, 9) surface predicts that a phase separation will occur between one reconstructed phase composed of 6.5 nm wide terraces with a discommensuration line parallel to the step and a nonreconstructed phase with terraces 1.4 nm wide. This is indeed in good agreement with our observations. This description gives all the physical arguments for interpreting, as a phase separation, the morphology of Au(1, 1, 1) vicinals with {1, 0, 0} steps, whose misorientation lies between 3° and 10°.

Now, we want to recall the faceted morphology of the Au(4, 5, 5) vicinal surface which presents the same misorientation angle as Au(11, 9, 9), but with {1, 1, 1} steps (i.e., misoriented towards the $[\bar{2}, 1, 1]$ azimuth) [7]. On such a surface, long range order distance of about 200 nm is observed. A phase separation schematically represented on Fig. 3a occurs between two vicinal phases: the largest terraces are reconstructed whereas the smallest are not. On the large terraces, the discommensuration lines, associated with the usual Au(1, 1, 1)-22 $\times$ $\sqrt{3}$ reconstruction, run perpendicular to and cross the steps, as schematically shown in Fig. 3a. The comparison between Figs. 3a and 3b clearly shows that the atomic arrangement is drastically different for both kinds of vicinal surfaces. In the following we examine how the atomic structure interplays with the mesoscopic order.

A theoretical approach to understand the periodicity of faceted surfaces has been proposed by Marchenko [8]. When a phase separation occurs on a vicinal surface, the discontinuities of the surface stress tensor at the edges between two facets generate lines of local forces which lead to long range bulk elastic relaxations. Marchenko demonstrated that in order to minimize the elastic energy, the surface morphology evolves towards the lowest possible period. However, there is a competition between this elastic energy gain and the local edge energy cost, C_1. The order of magnitude of the period is given by $\kappa = 2\pi a \exp(1 + C_1/C_2)$, where a is an atomic cutoff distance, and C_2 evaluates the bulk elastic relaxations [8].

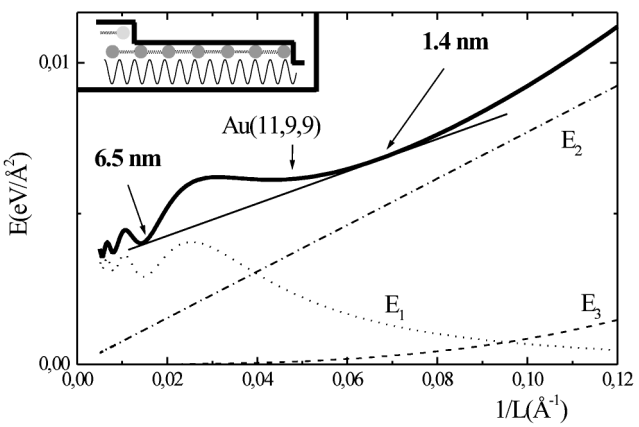

FIG. 2. Calculated energies per unit area of a Au(1, 1, 1) vicinal surface with {1, 0, 0} steps: total energy E, stressed terrace energy E_1, step energy contribution E_2, and elastic interaction between steps E_3. E_1 is calculated using the FK model schematically represented in the inset.

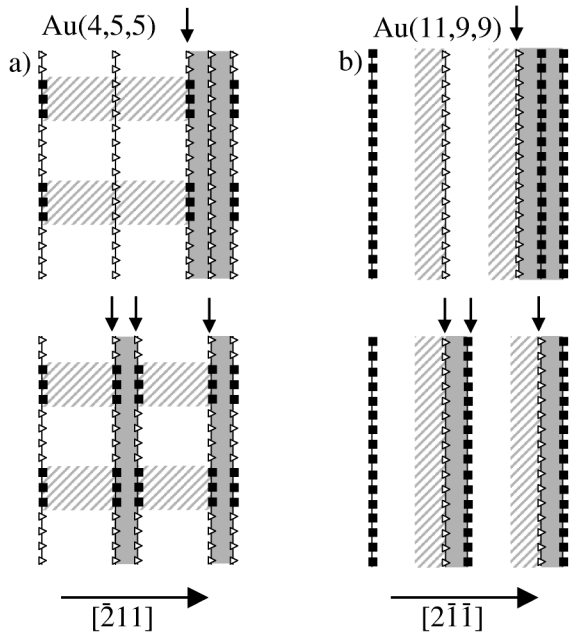

FIG. 3. Spontaneous periodic faceting of vicinals with {1, 1, 1} steps (a) and vicinals with {1, 0, 0} steps (b). In each case a schematic steps arrangement before (upper part) and after (lower part) one phase has been inserted into the other is drawn. The two terraces of the unreconstructed phase are in grey (i.e., they have an fcc stacking). The hcp atomic stacking fault on the two terraces of the reconstructed phase is represented by an hatched area. Arrows point out edges between vicinal phases. Step structures are indicated by triangles for {1, 1, 1} steps and full black squares for {1, 0, 0} steps.

In the case of Au(1, 1, 1) vicinals, the order of magnitude of C_2 has been previously estimated to be a few tenths of meV/Å, whatever the miscut azimuthal direction is [7]. The precise knowledge of the surface atomic structure allows us to estimate the local energy cost C_1 to insert one phase into the other. This insertion is schematically shown in Fig. 3 where step configurations are drawn before (upper part) and after (lower part) one phase has been inserted into the other. By definition, C_1 is the difference between the surface energies of the two configurations ignoring the elastic contribution which is already taken into account via the C_2 parameter. The term of first order is the difference in step energies. It can be seen in Fig. 3a that inserting one phase into the other for Au(4, 5, 5) transforms two {1, 1, 1} steps into a periodic succession of {1, 1, 1} and {1, 0, 0} step portions. Because of the higher step energy for the {1, 0, 0} steps, this results in a local energy cost C_1. An estimation of this term using the {1, 1, 1} and {1, 0, 0} step energies [17,18] as well as the proportion of hcp stacking along the step gives a few meV/Å. Following Marchenko's model, it leads to a micronic period for vicinal surfaces with {1, 1, 1} steps, not far from our observations of 200 nm. However, it is not expected to obtain a quantitative agreement, taking into account the roughness of our estimation together with the very high sensitivity of the exponential function. More interesting is the comparison with the Au(11, 9, 9) surface. Indeed, comparing steps in the upper and lower parts of Fig. 3b shows that no difference in step energies appears, when one phase is inserted into the other. In this case, additional effects must be invoked to evaluate C_1. It has been recently proposed that C_1 could result from the modification of the terrace widths in the vicinity of the frontier due to its asymmetric environment [19]. Following this work, we assumed a few percent variation of the edge terraces so that the edge energy cost can be evaluated from our Frenkel-Kontorova model. It is found to be a few tenth of meV/Å. This value is probably overestimated since the calculations of Liu *et al.* concern a much more asymmetric case than ours. However, this gives an upper limit for C_1 which is at the most equal to C_2. Thus, Marchenko's model predicts the smallest possible period that can be realized with the two favored terrace widths. This is indeed what we observe on the Au(11, 9, 9) surface. Of course, the validity of the Marchenko's model has to be discussed in the case of such a small phase extent but it is known that the elastic theory provides correct results until a few atomic distances. Therefore our results strongly suggest that the difference in C_1 between both type of vicinals is responsible for their drastically different mesoscopic faceted morphologies. Thus, Au(1, 1, 1) vicinal surfaces provide a unique opportunity to point out the crucial role played by the boundary energy cost in the self-organization phenomena. Surprisingly, although the edge energy cost is not the driving force for the periodic faceting, it is able to monitor the value of the period. This is indeed of primordial interest for numerous applications of self-organized systems.

As a conclusion, we have determined the precise atomic structure of some Au(1, 1, 1) vicinal surfaces. We have found completely different surface reconstructions depending on the azimuthal direction of miscut which lead to drastic changes for the periodicity of the faceted Au(1, 1, 1) vicinal surfaces. We have interpreted these results in the framework of elastic theory and demonstrated the crucial role of the boundary energy cost in the self-organization phenomena. This is an illustration of how the mesoscopic order can be governed by the microscopic arrangement. In order to monitor the mesoscopic order, several ways can be imagined to control the microscopic arrangement, such as reconstruction, temperature, or adsorbates. Thus this Letter opens the way to many studies and applications in self-organization physics.

This work has been supported by CNRS-ULTIMATECH PROGRAM, the CRIF, and the Université Paris 7.

[1] H. Brune *et al.,* Nature (London) **394**, 451 (1998).
[2] O. Fruchart *et al.,* Phys. Rev. Lett. **83**, 2769 (1999).
[3] F. Liu, J. Tersoff, and M. G. Lagally, Phys. Rev. Lett. **80**, 1268 (1998).
[4] J. Tersoff, C. Teichert, and M. G. Lagally, Phys. Rev. Lett. **76**, 1675 (1996), and references therein.
[5] V. A. Shchukin and D. Bimberg, Rev. Mod. Phys. **71**, 1125 (1999), and references therein.
[6] E. D. Williams, Surf. Sci. **299/300**, 502 (1994), and references therein.
[7] S. Rousset *et al.,* Surf. Sci. **422**, 33 (1999), and references therein.
[8] V. I. Marchenko, Sov. Phys. JETP **54**, 605 (1981).
[9] S. Rousset *et al.,* Surf. Sci. **443**, 265 (1999).
[10] J. V. Barth *et al.,* Phys. Rev. B **42**, 9307 (1990), and references therein.
[11] V. Repain *et al.,* Europhys. Lett. **47**, 435 (1999).
[12] B. Croset and C. de Beauvais, Surf. Sci. **384**, 15 (1997).
[13] M. Yoon *et al.,* Surf. Sci. **338**, 225 (1995).
[14] J. H. van der Merwe and C. A. B. Ball, in *Epitaxial Growth,* edited by J. W. Matthews (Academic, New York, 1975), Chap. 6.
[15] M. Mansfield and R. J. Needs, J. Phys. Condens. Matter **2**, 2361 (1990).
[16] B. Croset and C. de Beauvais, Phys. Rev. B **61**, 3039 (2000).
[17] Z. Wang and P. Wynblatt, Surf. Sci. **398**, 259–266 (1998).
[18] T. Michely and G. Comsa, Surf. Sci. **256**, 217 (1991).
[19] D. J. Liu and J. D. Weeks, Phys. Rev. Lett. **79**, 1694 (1997).